Surface Initiated ATRP of Acrylic Acid on Dopamine-Functionalized AAO Membranes

Wen-Cai Wang,[1] Jin Wang,[1] Yuan Liao,[1] Liqun Zhang,[1] Bing Cao,[1] Guojun Song,[2] Xilin She[2]

[1]*Key Laboratory of Carbon Fiber and Functional Polymers, Ministry of Education, and the Key Laboratory of Beijing City on Preparation and Processing of Novel Polymer Materials, Beijing University of Chemical Technology, Beijing 100029, People's Republic of China*
[2]*Institute of Polymer Materials, Qingdao University, Qingdao 266071, People's Republic of China*

Received 9 March 2009; accepted 11 June 2009
DOI 10.1002/app.30939
Published online 22 March 2010 in Wiley InterScience (www.interscience.wiley.com).

ABSTRACT: A facile method for surface-initiated atom transfer radical polymerization (ATRP) on the anodic aluminum oxide (AAO) membranes has been developed. The AAO membrane was firstly functionalized by poly (dopamine), the bromoalkyl initiator was then immobilized on the poly(dopamine) functionalized AAO membrane surface in a two-step solid-phase reaction, followed by ATRP of acrylic acid in a aqueous solution. The poly (acrylic acid) (PAAc)-grafted AAO membranes were characterized by X-ray photoelectron spectroscopy, fourier transform infrared spectroscopy and scanning electron microscopy. The XPS and FTIR results indicated that PAAc was successfully grafted on the AAO membrane surface. The degree of grafting increases linearly with the increase of monomer concentration, and it reaches a plateau when the reaction time up to 4 h. The results indicate that the thickness of the grafted polymer inside the isocylindrical pores of AAO membranes could be well controlled by changing the reaction time and monomer concentration. © 2010 Wiley Periodicals, Inc. J Appl Polym Sci 117: 534–541, 2010

Key words: ATRP; AAO; dopamine; graft copolymerization; XPS

INTRODUCTION

Mesoporous materials are a special type of nanomaterials with ordered arrays of uniform nanochannels. These materials have stimulated a lot of interest in the scientific community for the growth of monodisperse and ordered one-dimensional nanostructures within their pores.[1–4] These nanostructured materials have important applications in a wide variety of fields, such as separation, catalysis, adsorption, biotechnology, sensing technology, each of which demands different chemical and physical properties.[5–8] The realization of these devices will be dependent on the ability to modify and assemble nanoscale building blocks.

Surface initiated polymerization promised to be a versatile tool to further develop the chemical and physical properties of nanostructures, by providing a method to covalently attach polymer chains in a well-controlled fashion.[9] Especially, controlled/"living" free radical polymerization, such as atom transfer radical polymerization (ATRP), RAFT, etc, have a number of advantages over traditional polymerization procedures.[10,11] It has the ability to synthesize functionalized polymers with well-defined composition, structure, and a reasonably small polydispersity index, relative to the free radical process. ATRP has been used to grow polymers from a variety of substrates, including flat, convex, and concave surfaces, such as gold, magnetic nanoparticles, carbon nanotubes, silica, etc.[12–21] Depending on the geometry, the growing chains will experience different degrees of confinement that may ultimately affect the chain molecular weight and molecular weight distribution. Although confinement effects are not severe for small spheres, when polymer brushes are grown on flat or concave surfaces strong spatial restrictions exist. To date, most systems studied have involved polymer brushes on convex surfaces. However, literatures on the reporting of polymer brushes grown in concave surfaces are still limited.

In ATRP, there are two common approaches for the attachment of polymerization initiators.[10,11] The first approach relies on the reactions between end-functionalized initiator and native functional groups

Correspondence to: B. Cao (bcao@mail.buct.edu.cn).
Contract grant sponsor: The Beijing Nova Program; contract grant number: 2006B16.
Contract grant sponsor: The Major Project of Science and Technology Research from the Ministry of Education of China; contract grant number: 308003.
Contract grant sponsor: The Program for New Century Excellent Talents in University (NCET) (Ministry of Education of China).

originally present on the substrate surface.[12] A different approach involves the formation of a monolayer consisting of functional groups active toward the terminally functionalized (e.g., epoxide, amine, anhydride, or hydroxide) initiator.[15,19] Usually, the coupling methods are relatively complex and specific for certain substrate/initiator combinations. An alternative method for attachment of initiating functionalities to modified surface involves the deposition of a primary polymer (mono) layer with activity toward both surface and functionalized molecules. The polymer is used for the initial surface modification as well as for generation of the highly reactive primary layer. If the polymer used for building the primary layer contains functional groups, which are highly active in various chemical reactions, the primary layer approach becomes virtually universal toward both surface and end-functionalized initiating species being used for brush formation.

Recently, inspired by and studied on the composition of adhesive proteins in mussels, the adhesive mechanisms and adhesive behaviors of polydopamine have been reported.[22–23] The results indicate that dopamine (3, 4-dihydroxy-phenylalanine) and other catechol compounds perform well as binding agents for coating various substrates, including inorganic or organic materials. In this work, dopamine, as a bioinspired building block for surface coating, is used in the surface functionalization of anodic aluminum oxide (AAO) for the first time. The functionalized AAO is prepared via dipping the AAO membrane with dopamine aqueous solution for a period of time. Poly(dopamine) is formed and deposited on the inner wall of AAO as a permanent coating via the oxidation of dopamine by the oxygen dissolved in the solution. The catechol groups on poly(dopamine) could be readily used to immobilize the initiator.

The purpose of this article is two-fold. First, the effect of confinement imposed by concave geometry on surface-initiated polymerization is explored by using AAO as concave substrates. It also provide an alternative way to prepare one-dimensional polymer nanostructures by using AAO as a template. The polymeric nanotubes are characterized by close-packed, cylindrical nanopores that run straight through the thickness of the membrane and their tunable nanostructure has attracted great interest in electronic, optical, and sensing applications. The second objective is to explore the possibility of using dopamine functionalization as a general and simple method for ATRP initiator immobilization. Compared with the methods reported earlier, this spontaneous approach may provide a versatile way to immobilize ATRP initiators on various substrates and geometries.

EXPERIMENTAL

Materials

Anodic aluminum oxide (AAO) membranes with a nominal pore diameter of 200 nm and a thickness of 60 μm were purchased from Whatman Co. Ltd. 3-Hydroxytyramine hydrochloride (dopamine-HCl) was obtained from Aldrich Chemical Co. Tris (hydroxymethl aminomethane) was purchased from Alfa aesar Co. Acrylic acid was from Beijing Chemical Reagent Co., Ltd, and distilled under reduced pressure. Tetrahydrofuran (THF) was received from Beijing Chemical Reagent Co., Ltd, and dried by CaH_2, and distilled. Copper(I) chloride (CuCl, 98%) was supplied by Aldrich Chemical Co., dissolved in hydrochloric acid, precipitated into a large amount of deionized water, filtered, washed with anhydrous ethanol, and finally dried under reduced pressure at room temperature. 2,2-Dipyridyl was also purchased from Beijing Chemical Reagent Co., Ltd. All other solvents were obtained from Fisher Scientific Co. and were used as received. The chemical structure of dopamine is show as follows.

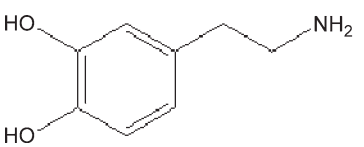

Dopamine

Dopamine self-polymerization and ATRP initiators immobilization

Poly(dopamine) self-polymerization on the AAO membranes surface were using a procedure similar to that has been described in the literature.[22] Briefly, 0.037 g dopa-HCl and 1.21 g tris were dissolved in 10 mL deioned water, and HCl was added to reach a pH of 8.5, then AAO membranes were dipped into the solution. pH-induced oxidation changes the solution color to dark brown. Stirring and/or vertical sample orientation was necessary to prevent nonspecific microparticle deposition on the surfaces. After deposition for 24 h, the membranes were rinsed by deionized water and dried by N_2. For the reaction of hydroxyl groups on the AAO-dopamine membrane with 2-bromoisobutyryl bromide (BIBB), the membranes were immersed in the anhydrous THF solution comprising 2-bromoisobutyryl bromide (BIBB, 10 m*M*) and triethylamine (10 m*M*) for 2 h. The BIBB reacts with the hydroxyl groups of the AAO-dopamine membrane to immobilize bromoester initiator groups covalently to the membrane surface. After the reaction, the initiator-functionalized membrane was removed from the reaction mixture and washed thoroughly with THF and deionized water before being dried under reduced pressure.

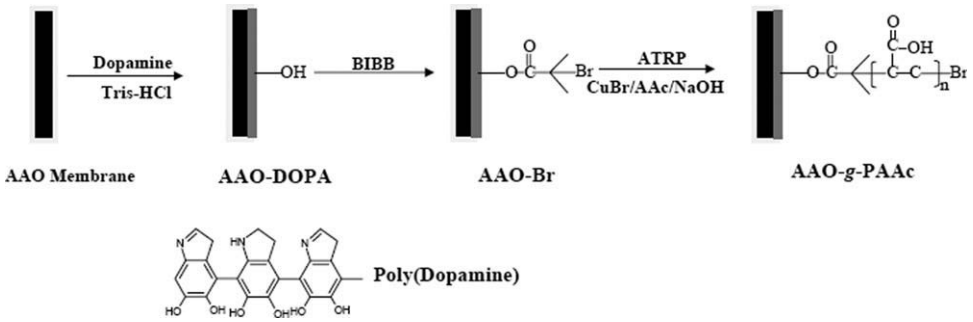

Figure 1 Schematic diagram illustrating the dopamine deposited AAO membrane, the initiator (BIBB) immobilized AAO membrane and the surface-initiated ATRP of AAc from the AAO-Br membranes.

Surface-initiated ATRP on the AAO-DOPA membranes

Surface-initiated atom transfer radical polymerization (ATRP) of PAA on the AAO-Br membrane was accomplished in a magnetically stirred glass tube (50 mL) by immersing the membrane into a reaction mixture. The reaction solution comprised the monomer, acrylic acid (AAc, 2.88 g, 1.0 mol/L); catalyst, CuBr (2.97 mg), 2,2-Dipyridyl (4.68 mg); and 40 mL of deionized water as solvent. AAc was deprotonated by the addition of NaOH to reach a pH end point of 10.2, followed by the addition of NaCl (5.59 g), according to the protocol first proposed by Sankhe et al.[24] The reaction mixture was purged with argon for 2 h in ice water bath to remove the dissolved oxygen. Polymerization was carried out at 50°C under argon atmosphere for the desired reaction time. At the end of the reaction, the poly(acrylic acid) (PAAc) graft AAO membrane (AAO-*g*-PAAc) was subjected to exhaustive washing and extraction with water and ethanol and then dried under reduced pressure at room temperature for at least 24 h until a constant weight was obtained.

Materials characterization

The surface chemical composition of the pristine and modified AAO membranes was characterized by X-ray photoelectron spectroscopy (XPS). The XPS measurements were performed on a Kratos AXIS HSi spectrometer using a Al K_α X-ray source (1486.6 eV photons) The X-ray source was run at a reduced power of 150 W (15 kV and 10 mA). The MF membranes were mounted on the standard sample studs by means of double-sided adhesive tapes. The core-level spectra were obtained at the photoelectron take-off angle (α, with respect to the sample surface) of 90°. The pressure in the analysis chamber was maintained at 10^{-8} Torr or lower during each measurement. To compensate for surface charging effects, all binding energies (BE's) were referenced to the C 1s hydrocarbon peak at 284.6 eV. In peak synthesis, the line width (full width at half maximum or FWHM) of Gaussian peaks was maintained constant for all components in a particular spectrum. Surface elemental stoichiometries were determined from the peak area ratios, after correction with the elementally determined sensitivity factors, and were accurate to within ±5%.

The surface and cross-sectional morphologies of the AAO membrane discs were imaged using a JEOL scanning electron microscope (SEM, model 5600LV). The membranes were mounted on the sample studs by means of double-sided adhesive tapes. A thin layer of platinum was sputtered on the sample surface before the SEM measurement. The SEM measurements were performed at an accelerating voltage of 20 kV.

Fourier transform infrared (FTIR) spectrum was collected in the transmission mode with Nicolet 750 under ambient conditions. Typically, 16 scans at a resolution of 4 cm^{-1} were accumulated to obtain one spectrum. The IR spectra were analyzed using the OMNIC 5.0 software.

RESULTS AND DISCUSSION

The process of surface functionalization of AAO membranes via controlled radical polymerization is shown in Figure 1: (i) poly(dopamine) was deposited on the AAO membrane and inside the pore surfaces to introduce catechol groups onto the membrane (hereafter refer to the AAO-DOPA surface), (ii) the catechol groups on the AAO-DOPA membrane react with BIBB led to the alkyl halide-functionalized AAO-Br membrane (hereafter refer to the AAO-Br surface), and (iii) consecutive surface-initiated ATRP from the AAO-Br membrane (hereafter refer to the AAO-*g*-PAAc surface). The details involved in each reaction step are discussed below.

Surface functionalization of AAO membranes by dopamine self-polymerization and the initiator immobilization

To initiate the ATRP polymerization on the AAO membrane surface, a uniform layer of initiators

immobilized on the AAO membrane and its pore surface is indispensable. In this work, a two step process was developed for the immobilization of ATRP initiators on the AAO membrane: (1) Dopamine was firstly deposited on to the surface of AAO membranes to introduce the catechol groups. (2) The reaction of the catechol groups on the AAO membrane with BIBB to produce the alkyl bromide-terminated AAO-Br surface.

To date, the physicochemical details of dopamine-surface interaction and the mechanism for dopamine self-polymerization was kept unknown. Lee et al. reported the single-molecule mechanics of mussel adhesion. It is likely to involve oxidation of the catechol to a quinone, followed by polymerization in a manner reminiscent of melanin formation, which occurs through polymerization of structurally similar compounds.[22,23] The observed color transfer from light pink to deep dark in the dopamine coating process indicate the polymerization may follow by a reaction in a manner of melanin formation. As suggested by Lee et al., under an oxidative condition, e.g., alkaline pH, dihydroxyl group protons in dopamine are deprotonated, becoming dopamine-quinone, which subsequently rearranges via intramolecular cyclization to leukodopaminechrome. Further oxidation and rearrangement leads to 5,6 dihydroxyindole, whose further oxidation causes intermolecular crosslinking to yield a polymer that is structurally similar to the bio-pigment melanin. In this work, the success of modification of AAO membranes with dopamine followed with initiator immobilization was ascertained by comparing the XPS spectra of the pristine and modified membranes. Figure 2 shows the respective wide scan and N 1s core level spectra of the pristine AAO membrane [Fig. 2(a,b)], the AAO-DOPA membrane [Fig. 2(c,d)], and the initiator immobilized AAO surface (AAO-Br) [Fig. 2(e,f)]. The spectrum of the pristine AAO membrane showed four main signals corresponding to C 1s (284.6 eV), O 1s (532 eV), Al 2p (73 eV), and Al 2s (118 eV). The carbon-containing groups on the surface of the AAO arise from the organic chemicals used in the preparation of these membranes. The presence of the poly(dopamine) on the AAO-DOPA surface can be deduced from the appearance of the new peak components with the BE at 399.5 eV, associated with the amine species of dopamine, as shown in Figure 2(c,d). The [C—O]/[C] and [C—N]/[C] ratio, as determined from the curve-fitted C 1s core-level spectrum, is about 0.27 and 0.12, respectively, in agreement with the theoretical ratio for the poly(dopamine). The nitrogen to carbon signal ratio (N/C) for the AAO-DOPA surface is 0.06, which is lower than that of the theoretical value for dopamine (N/C = 0.125), implying that the thickness of the self-polymerized dopamine layer is below the probing depth of the XPS technique (about 7.5 nm for an organic matrix).[25]

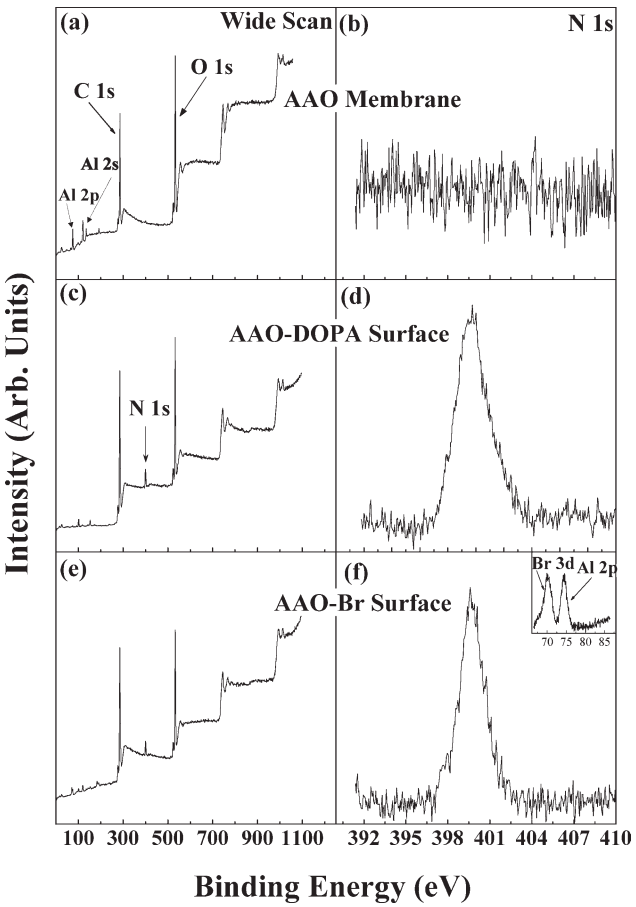

Figure 2 XPS wide scan and N 1s core level spectra of (a) the pristine AAO membrane, (b) the AAO-DOPA membrane, and (c) the AAO-Br surface.

A comparison of the wide-scan spectra of the AAO-DOPA [Fig. 2(c,d)] and AAO-Br membrane surfaces [Fig. 2(e,f)] reveals that the Br 3d (at a BE of about 69 eV), Br 3p (at a BE of about 182 eV), and Br 3s (at a BE of about 256 eV) signals, characteristic of covalently bonded bromine, have appeared on the AAO-Br surface.[26] The corresponding Br 3d core-level spectrum is shown in the insert of Figure 2(f). Whereas a strong Al 2p peak is shown besides the Br 3d peak, indicating that the thickness of the thickness of the initiator and poly(dopamine) layer is below the probing depth of the XPS technique. The surface [Br]/[N] ratio, determined from the sensitivity factor-corrected Br 3d and N 1s core-level spectra area ratio, is 0.57, provides a direct measure of the concentration of initiators in the surface region. The surface [Br]/[N] ratios did not vary significantly when different locations of the membrane surface were measured, indicating a uniform distribution of the initiator across the membrane surface.

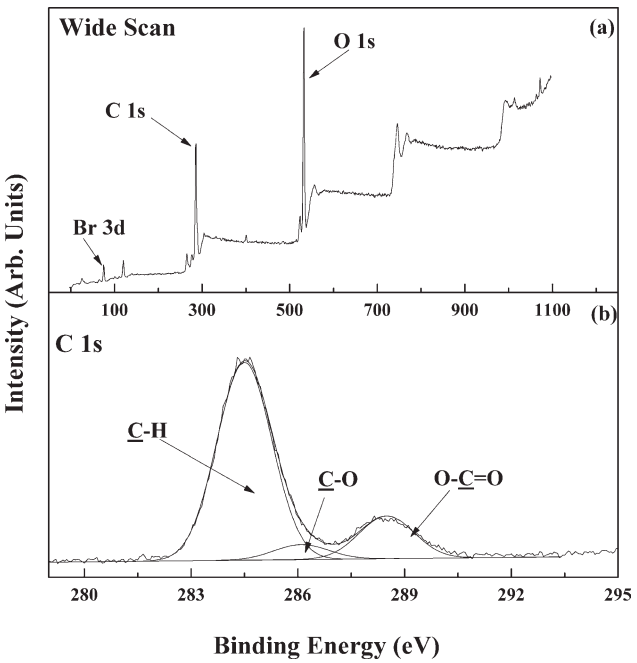

Figure 3 XPS wide scan and C 1s core level spectra of the AAO-*g*-PAAc membrane (ATRP time of 3 h and AAc concentration of 1 *M*).

Surface-initiated ATRP of AAc on the AAO-Br membranes

The physicochemical properties of the AAO membrane and its pore surfaces can be tuned by the grafting of functional polymer brushes. In this work, acrylic acid (AAc) was selected as the model monomer for the preparation of functional polymer brushes from the AAO-Br membranes via surface initiated ATRP. In surface-initiated ATRP, the initiator concentration on a surface is usually low compared with that used for bulk or solution ATRP. To quickly establish an equilibrium between dormant and active chains during surface-initiated ATRP, an excess amount of deactivating Cu(II) complex was added. This approach allows thicker polymer brushes to be grown at a faster rate in the presence of a higher monomer concentration because of the absence of accompanying homo-polymerization (nontethered polymerization) in solution.

The presence of grafted PAAc on the AAO-Br membrane surfaces was confirmed by XPS analysis after the surfaces had been subjected to vigorous washing and extraction. Figure 3 shows the wide-scan and C 1s core-level spectra of the AAO-*g*-PAAc (from 3 h of ATRP), respectively. In comparison with the wide-scan spectrum of the AAO-Br membrane surface [Fig. 2(e)], the N 1s signal (at a BE of about 399 eV) in the wide-scan spectra of the AAO-*g*-PAAc membrane surfaces has almost disappeared. As shown in Figure 3(b), the C 1s core-level spectra of the AAO-*g*-PAAc membrane surfaces can be curve-fitted into three peak components, with BEs at 284.6 for the C—H species, at 286.2 eV for the C—O species and at 288.4 eV for the O—C=O species, respectively. The XPS results indicate that the densely grafted PAAc brushes have covered the membrane completely to a thickness exceeding the sampling depth of the XPS technique.[25]

Chemical structure of the membranes characterization by FTIR

The chemical structure of the AAO membranes was also investigated by FTIR spectroscopy. Figure 4 shows the respective FTIR spectrum of the pristine AAO-DOPA membrane [Fig. 4(a)], the DOPA-Br

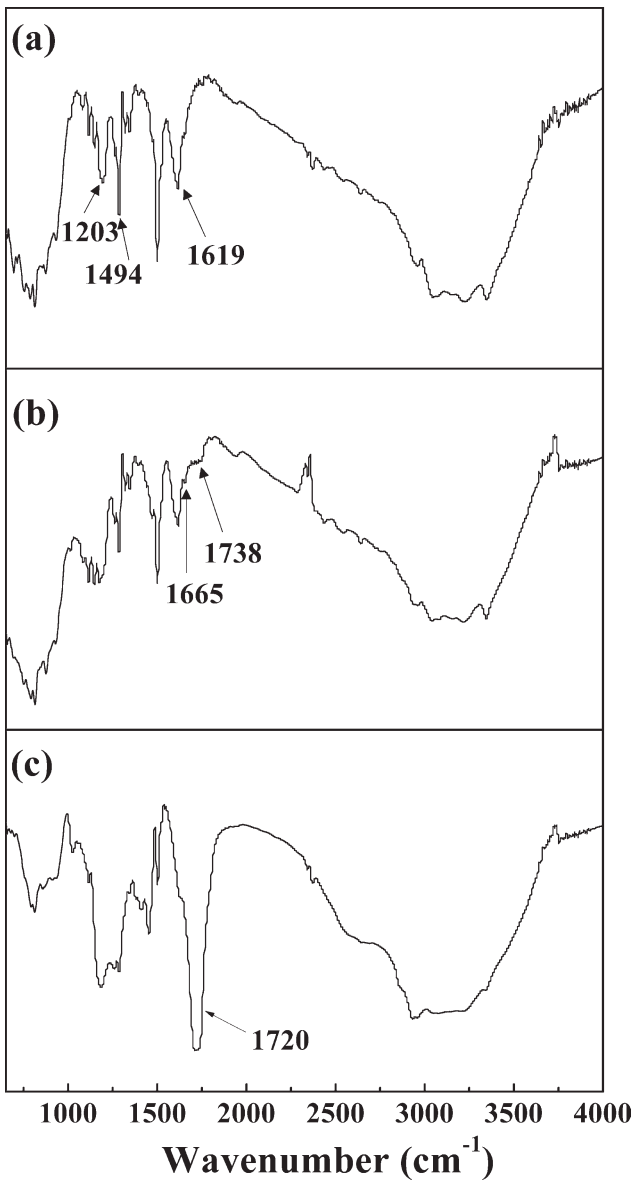

Figure 4 FTIR spectra of (a) the AAO-DOPA membrane, (b) the AAO-Br membrane and (c) AAO-*g*-PAAc membrane (ATRP time of 3 h, and AAc concentration of 1M).

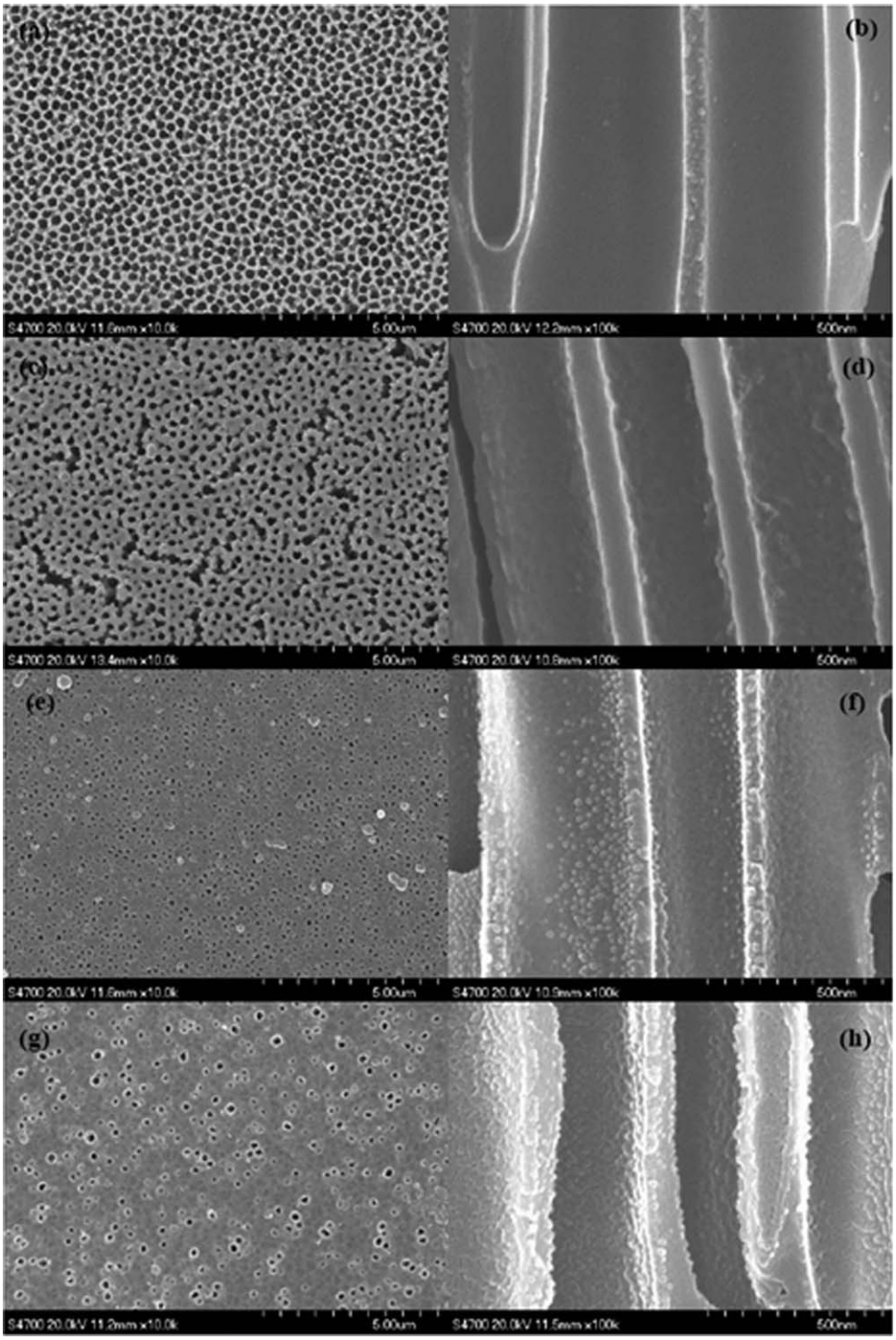

Figure 5 SEM images of the top and cross-sectional views of (a, b) the pristine AAO membrane, (c, d) the AAO-DOPA membrane, (e, f) the AAO-*g*-PAAc membrane (ATRP time of 3 h), (g, h) the AAO-*g*-PAAc membrane (ATRP time of 6 h).

membrane [Fig. 4(b)] and the AAO-*g*-PAAc membrane [Fig. 4(c)]. In Figure 4(a), the broad absorption bands at 3000–3400 cm^{-1} are due to stretching of the —OH and $—NH_2$ groups of poly(dopamine). The adsorption peak in the region of 900–1000 cm^{-1} is due to the C—H bending vibrations on the benzene ring, and 1494 and 1203 cm^{-1} is due to the C=C and C—O stretching vibration of the benzene ring. The adsorption peak at wavenumber of 1619 cm^{-1} is due to the N-H stretching of the primary amine in the poly(dopamine) structure. In Figure 4(b), after the initiator of BIBB has been attached, the peak intensity at 1203, 1287, and 1619 cm^{-1}, which due to OH and NH_2 groups, are weakened. There is a protuberance in 1665 and 1738 cm^{-1} represent the C=O stretching vibration of the N—C=O and O—C=O

groups, respectively. These results show that the initiator BIBB is reacted with poly(dopamine), as a result, successfully immobilized onto the membrane surface. It can be seen from Figure 4(c) that the strong peak at 1720 cm^{-1}, attributed to the C=O stretching vibrations, suggest that PAAc has successfully grafted onto the AAO membranes via ATRP process. The FTIR results are thus in consist with the XPS results shown in Figure 2 and 3.

Surface topography of the AAO membranes

The surface morphology of the AAO membranes at various stages of surface modification was studied by SEM. Figure 5 shows the respective SEM images of the top and cross-sectional views of the pristine AAO membrane [Fig. 5(a,b)], the AAO-DOPA membrane [Fig. 5 (c,d)], an AAO-*g*-PAAc membrane following 3 h of ATRP [Fig. 5(e,f)], and an AAO-*g*-PAAc membrane following 6 h of ATRP [Fig. 5(g,h)]. Obviously, the AAO membrane has symmetrical distributing micropores, and the diameter of the micropores was about 250 nm. The internal surface of the micropores is smooth. After the poly(dopamine) deposition, it can be seen from Figure 5(c,d) that there was a uniform polymer layer deposited on the membrane surface and inside the micropores. The thickness of the poly(dopamine) layer is in the range of about 20–30 nm, indicating that the poly (dopamine) was successfully deposited onto the AAO membrane. It should be mentioned here that there is no obvious change in the surface and internal morphologies of the AAO membranes after initiator immobilization (not shown here). After the graft polymerization of AAc, the membrane pores become smaller than those of the starting AAO-Br membrane [Fig. 5(e,f)]. Obviously, there were many particles on the inside of the pore surface. With the increase in polymerization time, the pore sizes decrease further, consistent with the presence of denser and longer surface-grafted AAC brushes. The cross- sectional SEM images of the membranes also indicated that graft polymerizations have occurred throughout the pore surfaces.

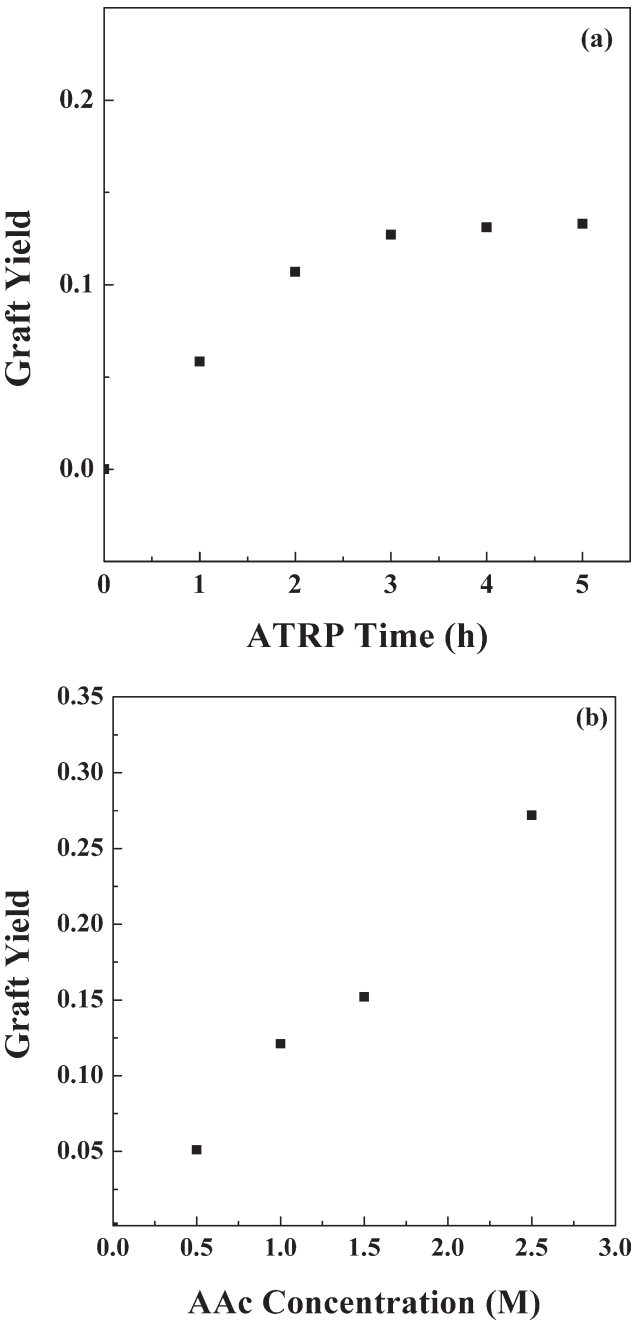

Figure 6 Dependence of graft yield of the AAO-*g*-PAAc membranes on: (a) the surface-initiated ATRP time, and (b) the AAc concentration.

Kinetics of the ATRP grafting process

The kinetics of PAAc growth from the AAO-Br membranes via surface-initiated ATRP was investigated. The grafting yield (GY) was determined gravimetrically, the graft concentration can be defined as following:

GY = (Wight of AAO-*g*-PAAc—Weight of AAO-Br)/Weight of AAO-Br

Figure 6(a,b) show the dependence of the grafting yield on the ATRP time and monomer concentration, respectively. It can be seen that the degree of grafting increases with polymerization time for modification times up to 4 h, and it reaches a plateau degree of grafting for longer polymerization times. The results suggest that the chain growth from the AAO-Br membrane is consistent with a living and well-defined process. The nonlinear growth behavior has been described for other polyacids, including poly (methacrylic acid), and results from chain termination reactions, as well as catalyst deactivation.[27,28] Add alkali salt in the reaction system, such as NaCl,

which suppresses the ion-exchange reactions that otherwise lead to complexation between the catalyst and monomer and the dissociation of the Cu(II) species that forms during the ATRP process. Thus, catalyst deactivation can be excluded, and the non-linear growth observed for our system is most likely attributed to bimolecular chain termination. The relationship between the grafting yield and the monomer concentration is shown in Figure 6(b). An approximately linear increase in grafting yield of the PAAc chains on the AAO-Br membranes with the AAc monomer concentration, suggest that the growth of the PAAc chains was a controlled process, which is consisted with the results reported by Sankhe et al.[24] Control experiments on the pristine AAO and AAO-DOPA membranes revealed that there was no increase in graft yield when they were subjected to the "surface initiated" ATRP of AAc under similar reaction conditions. All of these results are consistent with the successful graft polymerization of AAc on the AAO-Br membranes via surface-initiated ATRP. Another unique characteristic of polymers synthesized by ATRP is the preservation of initiation groups at the chain ends. As it has been shown in the XPS results in Figure 3(a), polymers synthesized by ATRP still retain the terminal alkyl halides. The dormant PAAc chain ends can be reactivated to serve as macroinitiators for the subsequent growth of a second polymer block.

CONCLUSIONS

A novel two-step process was developed for the immobilization of ATRP initiators on the AAO membrane and its pore surfaces. The immobilized initiators allowed well-defined functional polymer PAAc to be covalently grafted onto the pore surface of the AAO membrane via surface-initiated ATRP. The kinetics study revealed an approximately linear increase in the graft yield of the PAAc with polymerization concentration, indicating that chain growth from the membrane surface was consistent with a controlled process. With the development of a simple approach to the covalent immobilization of ATRP initiators on AAO and the inherent versatility of surface initiated ATRP, the surface functionality of AAO membranes could be precisely tailored in a controlled manner.

References

1. Xia, Y. N.; Yang, P. D.; Sun, Y. G. Adv Mater 2003, 15, 353.
2. Martin, C. R. Acc Chem Res 1995, 28, 61.
3. Yanagishita, T.; Nishio, K.; Masuda, H. Adv Mater 2005, 17, 2241.
4. Prieto, A. L.; Martin, M. G.; Keyani, J.; Gronsky, R.; Sands, T.; Stacy, A. M. J Am Chem Soc 2003, 125, 2388.
5. Martin, C. R. Science 1994, 266, 961.
6. Burda, C.; Chen, X.; Narayanan, R.; Ei-Sayed, M. A. Chem Rev 2005, 105, 1025.
7. Wilson, O.; Wilson, G. J.; Mulvaney, P. Adv Mater 2002, 14, 1000.
8. Wang, Y. J.; Angelatos, A. S.; Caruso, F. Chem Mater 2008, 20, 848.
9. Kato, K.; Uchida, E.; Kang, E. T.; Uyama, Y.; Ikada, Y. Prog Polym Sci 2003, 28, 209.
10. Matyjaszewski, K.; Xia, J. H. Chem Rev 2001, 101, 2921.
11. Goto, A.; Fukuda, T. Prog Polym Sci 2004, 29, 329.
12. Carlmark, A.; Malmstrom, E. E. Biomacromolecules 2003, 4, 1740.
13. Burkett, S. L.; Ko, N.; Stern, N. D.; Caissie, J. A.; Sengupta, D. Chem Mater 2006, 18, 5137.
14. Fan, X. W.; Lin, L. J.; Messermith, P. B. Biomacromolecules 2006, 7, 2443.
15. Xu, C.; Wu, T.; Mei, Y.; Drain, C. M.; Batteas, J. D.; Beers, K. L. Langmuir 2005, 21, 11136.
16. Huang, W.; Kim, J. B.; Bruening, M. L.; Bake, G. L. Macromolecules 2002, 35, 1175.
17. Hester, J. F.; Banerjee, P.; Won, Y. Y.; Akthakul, A.; Acar, M. H.; Mayes, A. M. Macromolecules 2002, 35, 7652.
18. Xu, F. J.; Li, Y. L.; Kang, E. T.; Neoh, K. G. Biomacromolecules 2005, 6, 1759.
19. Plunkett, K. N.; Zhu, X.; Moore, J. S.; Leckband, D. E. Langmuir 2006, 22, 4259.
20. Kong, H.; Gao, C.; Yan, D. Y. J Am Chem Soc 2004, 126, 412.
21. Rupert, B. L.; Mulvihill, M. J.; Arnold, J. Chem Mater 2006, 18, 5045.
22. Lee, H.; Dellatore, S. M.; Miller, W. M.; Messersmith, P. B. Science 2007, 318, 426.
23. Lee, H.; Lee, B. P.; Messersmith, P. B. Nature 2007, 448, 338.
24. Sankhe, A. Y.; Husson, S. M.; Kilbey, S. M. J Polym Sci Part A: Polym Chem 2007, 45, 566.
25. Tan, K. L.; Woon, L. L.; Kang, E. T.; Neoh, K. G. Macromolecule 1993, 26, 2832.
26. Beamson, G.; Briggs, D. High Resolution XPS of Organic Polymers: the Scienta ESCA300 Database; John Wiley: New York, 1992, p 214.
27. Sankhe, A. Y.; Husson, S. M.; Kilbey, S. M. Macromolecules 2006, 39, 1376.
28. Singh, N.; Wang, J.; Ulbricht, M.; Wickramasinghe, S. R.; Husson, S. M. J Membrane Sci 2008, 309, 64.